© 2015. Published by The Company of Biologists Ltd | The Journal of Experimental Biology (2015) 218, 1478-1486 doi:10.1242/jeb.118570

RESEARCH ARTICLE

Characterization of the target of ivermectin, the glutamate-gated chloride channel, from *Anopheles gambiae*

Jacob I. Meyers[1,*], Meg Gray[2], Wojtek Kuklinski[2], Lucas B. Johnson[3], Christopher D. Snow[3], William C. Black IV[2], Kathryn M. Partin[1] and Brian D. Foy[2]

ABSTRACT

The use of insecticide-treated nets and indoor residual insecticides targeting adult mosquito vectors is a key element in malaria control programs. However, mosquito resistance to the insecticides used in these applications threatens malaria control efforts. Recently, the mass drug administration of ivermectin (IVM) has been shown to kill *Anopheles gambiae* mosquitoes and disrupt *Plasmodium falciparum* transmission in the field. We cloned the molecular target of IVM from *A. gambiae*, the glutamate-gated chloride channel (AgGluCl), and characterized its transcriptional patterns, protein expression and functional responses to glutamate and IVM. AgGluCl cloning revealed an unpredicted fourth splice isoform as well as a novel exon and splice site. The predicted gene products contained heterogeneity in the N-terminal extracellular domain and the intracellular loop region. Responses to glutamate and IVM were measured using two-electrode voltage clamp on *Xenopus laevis* oocytes expressing AgGluCl. IVM induced non-persistent currents in AgGluCl-a1 and did not potentiate glutamate responses. In contrast, AgGluCl-b was insensitive to IVM, suggesting that the AgGluCl gene could produce IVM-sensitive and -insensitive homomultimers from alternative splicing. AgGluCl isoform-specific transcripts were measured across tissues, ages, blood feeding status and sex, and were found to be differentially transcribed across these physiological variables. Lastly, we stained adult, female *A. gambiae* for GluCl expression. The channel was expressed in the antenna, Johnston's organ, supraesophageal ganglion and thoracic ganglia. In summary, we have characterized the first GluCl from a mosquito, *A. gambiae*, and described its unique activity and expression with respect to it as the target of the insecticide IVM.

KEY WORDS: *Anopheles gambiae*, Ivermectin, Glutamate-gated chloride channel

INTRODUCTION

The 2014 WHO World Malaria Report (available at: http://www.who.int/malaria/publications/world_malaria_report_2014/en/) estimates that in 2013 there were 198 million cases worldwide causing 584,000 malaria-related deaths. Nearly 90% of these deaths occurred in Africa where a primary vector of malaria is *Anopheles gambiae sensu stricto* (s.s.) (WHO World Malaria Report, 2014). Current malaria control programs primarily target malaria vectors through the use of long-lasting insecticide-treated bed nets and indoor residual spraying of pyrethroid-based insecticides. However, pyrethroid resistance is becoming widespread in many *A. gambiae* populations across Africa (Ranson et al., 2011; Trape et al., 2011). Out of the recent efforts to find new vector-targeting interventions with novel modes of action, the endectocide ivermectin (IVM) has arisen as a new candidate to control malaria transmission. IVM, when imbibed by vectors from host-treated blood meals, has proven to efficiently kill or disable *A. gambiae* s.s. both in the lab and in the field (Kobylinski et al., 2010; Sylla et al., 2010). More recently, IVM mass drug administration in multiple locations across West Africa has been shown to temporarily reduce the proportion of *Plasmodium falciparum*-infected *A. gambiae* in IVM-treated villages (Kobylinski et al., 2011; Alout et al., 2014). Sub-lethal doses of IVM have also been shown to inhibit the sporogony of *P. falciparum* in *A. gambiae* s.s. and impair coordinated flight patterns (Butters et al., 2012; Kobylinski et al., 2012). In clinical trials, IVM, in combination with artemether-lumefantrine, has been shown to reduce the likelihood of malaria transmission through reduction of mosquito survivorship (Ouedraogo et al., 2014). These studies demonstrate that IVM has promise as a novel malaria control tool.

The primary target of IVM is the invertebrate glutamate-gated chloride channel (GluCl) (Cully et al., 1994, 1996; Janssen et al., 2007, 2010; McCavera et al., 2009; Moreno et al., 2010), though it also has efficacy against other members of the invertebrate Cys-loop family of neurotransmitter receptors including the γ-aminobutyric acid- (Brown et al., 2012), histamine- (Zheng et al., 2002) and pH-sensitive chloride channels (Schnizler et al., 2005). Because IVM is used to control and treat parasitic nematode diseases (Õmura, 2008), the majority of research on IVM targets has occurred in nematodes or model organisms, but the function of GluCl in mosquito disease vectors is unknown.

The purpose of this study was to characterize GluCl from *A. gambiae* Giles 1902 in order to understand the physiological role of GluCl and how IVM may be affecting mosquito physiology. Cloning of the *A. gambiae* GluCl (AgGluCl) revealed unique splicing sites and products not previously predicted. We expressed AgGluCl clones in *Xenopus laevis* oocytes to measure its electrophysiological activity in response to glutamate and IVM. We also examined AgGluCl isoform-specific transcript levels across different tissues, ages, blood-feeding status and sex and GluCl tissue expression in adult *A. gambiae*.

RESULTS

Cloning of AgGluCl splice isoforms and gene structure

We identified the putative *A. gambiae* GluCl (AgGluCl) gene using the basic local alignment search tool (BLAST) algorithm on the VectorBase Community Annotation Database (https://www.vectorbase.org/) (Megy et al., 2012). We probed the *A. gambiae* genome for similar DNA sequences to the GluCl coding sequences

[1]Department of Biomedical Sciences, Colorado State University, 1617 Campus Delivery, Fort Collins, CO 80523-1617, USA. [2]Arthropod-borne and Infectious Diseases Laboratory, Department of Microbiology, Immunology and Pathology, Colorado State University, 1692 Campus Delivery, Fort Collins, CO 80523-1692, USA. [3]Department of Chemical and Biological Engineering, Colorado State University, 1370 Campus Delivery, Fort Collins, CO 80523-1370, USA.

*Author for correspondence (Jacob.I.Meyers@gmail.com)

Received 18 December 2014; Accepted 24 March 2015

The Journal of Experimental Biology

The Journal of Experimental Biology (2015) 218, 1478-1486 doi:10.1242/jeb.118570

from *Caenorhabditis elegans* (CeGluClα) (Cully et al., 1994) and *Drosophila melanogaster* (DmGluClα) (Cully et al., 1996) (supplementary material Fig. S1). Sequence analysis revealed one significant hit in the *A. gambiae* PEST strain genomic sequence (AGAP001434; Assembly: AgamP4). This gene was cloned out of a cDNA library created from mRNA isolated from adult blood-fed female *A. gambiae*.

Vectorbase predicts AgGluCl (AGAP001434) contains 10 exons with exon 3 being alternatively spliced to produce three splice isoforms (https://www.vectorbase.org/) (Megy et al., 2012). However, our cloning resulted in the discovery of four splice isoforms containing DNA coding sequences not predicted by Vectorbase (Fig. 1A). The newly discovered splice isoform contains the same splicing pattern as the 'AgGluCl-a' named currently in Vectorbase (inclusion of exon 3a and splicing out of exons 3b and 3c), but incorporates additional nucleotide sequences. We propose renaming 'AgGluCl-a' as AgGluCl-a1 and naming the new splice isoform AgGluCl-a2.

We discovered two additional DNA sequences that are incorporated into the AgGluCl coding sequence that were not previously predicted. The first of these sequences is a small 15 nt sequence found only in AgGluCl-b (nt position 1007–1021). When we searched the Vectorbase genomic data for this sequence, we discovered it at the intron/exon junction of intron 7 and exon 8. Our data show that this sequence is spliced out of AgGluCl-a1, -a2 and -c, but included in splice isoform b. The second sequence is a 33 nt insertion found in the novel splice isoform AgGluCl-a2 and in AgGluCl-b. Positional analysis of this insertion showed that it occurs in predicted intron 9, between exons 9 and 10 (position 901–933). This sequence, previously predicted to be part of intron 9, is actually a novel exon. These findings redefine the structure of the AgGluCl gene to incorporate an additional exon (exon 10) and change the overall number of AgGluCl exons to 11 (Fig. 1A).

AgGluCl splice isoform protein structure

Analysis of the putative AgGluCl gene products revealed a protein corresponding with chloride-permeable members of the Cys-loop family of neurotransmitter receptors. Members of this family contain a signal peptide, a large N-terminal extracellular domain with two conserved disulfide bonds, four transmembrane domains, an anion-permeable pore and a large intracellular loop between transmembrane regions 3 and 4 (Fig. 1B,C). ClustalW alignment of the gene product with the recently crystallized GluClα from *C. elegans* (CeGluCl) and *D. melanogaster* GluCl (DmGluCl) revealed a protein with conserved residues associated with the glutamate and IVM binding pockets (supplementary material Fig. S1) (Hibbs and Gouaux, 2011).

AgGluCl splice isoforms contain two major regions of heterogeneity in the protein structure. The first results from the alternative splicing of exons 3a, 3b and 3c. This encodes a 22 amino acid region found on the N-terminal extracellular domain of the channel. This region contains loop G of the glutamate binding pocket (Fig. 1B,C) (Hibbs and Gouaux, 2011). The second region of heterogeneity is the result of alternatively spliced exon 8 (five amino acids) and exon 10 (11 amino acids). The products of these alternative splicing events occur within the large intracellular loop between transmembrane domains 3 and 4 (Fig. 1C). The splicing product of exon 8 is found immediately after transmembrane domain 3 and the splicing product of exon 10 is found prior to transmembrane domain 4. All GluCl crystal structures required the removal of this intracellular loop for crystallization, which is why it was not included in our AgGluCl homology model (Fig. 1B).

Functional expression and activity of AgGluCl

Heterologous expression of *A. gambiae* receptors and electrophysiological analysis pose technical challenges, but are important to understanding the physiological responses of a newly cloned channel. Previous attempts to heterologously express and functionally characterize other members of the Cys-loop family from *A. gambiae* have been unsuccessful (Jones et al., 2009). In this study, *Xenopus laevis* oocytes were injected with AgGluCl mRNA and incubated for 72–120 h for protein expression. Sufficient AgGluCl expression to permit measurable currents was successful for less than 5% of oocytes injected with AgGluCl mRNA. In oocytes expressing functional AgGluCl-b, glutamate evoked a rapidly activating inward current. AgGluCl-b responses were analyzed for glutamate concentrations ranging from 10 to 300 µmol l^{-1} (Fig. 2A). A dose–response curve was fitted to the data using the Hill equation. The EC_{50} for glutamate was 30.22±2.75 µmol l^{-1} and the Hill coefficient was 1.93±0.32, suggesting that more than one glutamate molecule is necessary to activate the channel (Fig. 2B). AgGluCl-b was insensitive to IVM (Fig. 2C).

IVM induced a slowly activating current in oocytes expressing AgGluCl-a1 (Fig. 2C). The peak current activated by 10 µmol l^{-1} IVM was 208.1±60.8% (mean±s.d., N=5) greater than the peak current activated using the highest tested glutamate concentration (300 µmol l^{-1}). IVM did not potentiate subsequent glutamate-evoked current in AgGluCl-a1 when compared with control (114.3±16.1%, mean±s.d., N=5). We were not successful at expressing AgGluCl-a2 or AgGluCl-c.

Transcriptional profile of AgGluCl splice isoforms in adult *A. gambiae*

We measured AgGluCl isoform-specific transcript levels relative to the housekeeping gene ribosomal protein S7 (RPS7) across tissues, ages, blood-feeding status and sex (Fig. 3). When total AgGluCl transcripts (all isoforms together) were analyzed by blood-feeding status and age, the act of blood feeding significantly, but modestly, reduced total transcript levels in 3 days post-emergence (dpe) adult females (P<0.0001, N=3), but not in those at 7 dpe (P=0.6005, N=3) or 15 dpe (P=0.9742, N=3). The addition of IVM to a blood meal significantly increased AgGluCl transcript levels in 3 dpe females (P<0.0001, N=3), but not in 7 dpe (P=0.9919, N=3) or 15 dpe (P=0.7133, N=3) females (Fig. 3A). Adult female *A. gambiae* had significantly lower AgGluCl transcript levels when compared with males at 3 dpe (P<0.0001, N=3) and 15 dpe (P<0.0001, N=3) and approximately equal AgGluCl transcript levels at 7 dpe (P=0.4158, N=3) (Fig. 3A).

Analysis of AgGluCl tissue-specific expression revealed transcripts primarily in the head and thorax, with the highest transcript levels found in the head. This tissue-specific expression pattern was consistent across all ages, blood-feeding status and sex except one (P<0.05 for all head versus thorax comparisons except 3 dpe blood fed, head versus thorax: P=0.6519, N=3) (Fig. 3B). We detected no AgGluCl transcripts in the female abdomen until 15 dpe, the oldest age tested, while AgGluCl transcripts were always present in low levels in the male abdomen. The abdominal AgGluCl transcripts at 15 dpe were of relatively low abundance and predominately the AgGluCl-c isoform (Fig. 3B,C).

Analysis of isoform-specific expression patterns showed that the predominant AgGluCl isoforms were AgGluCl-a (our assay could not distinguish these related isoforms, the transcripts could be either AgGluCl-a1 or -a2) and AgGluCl-b (Fig. 3C). Transcripts of these isoforms are found in relatively equal amounts across tissues, ages and blood-feeding status. AgGluCl-c transcripts were found at very

The Journal of Experimental Biology (2015) 218, 1478-1486 doi:10.1242/jeb.118570

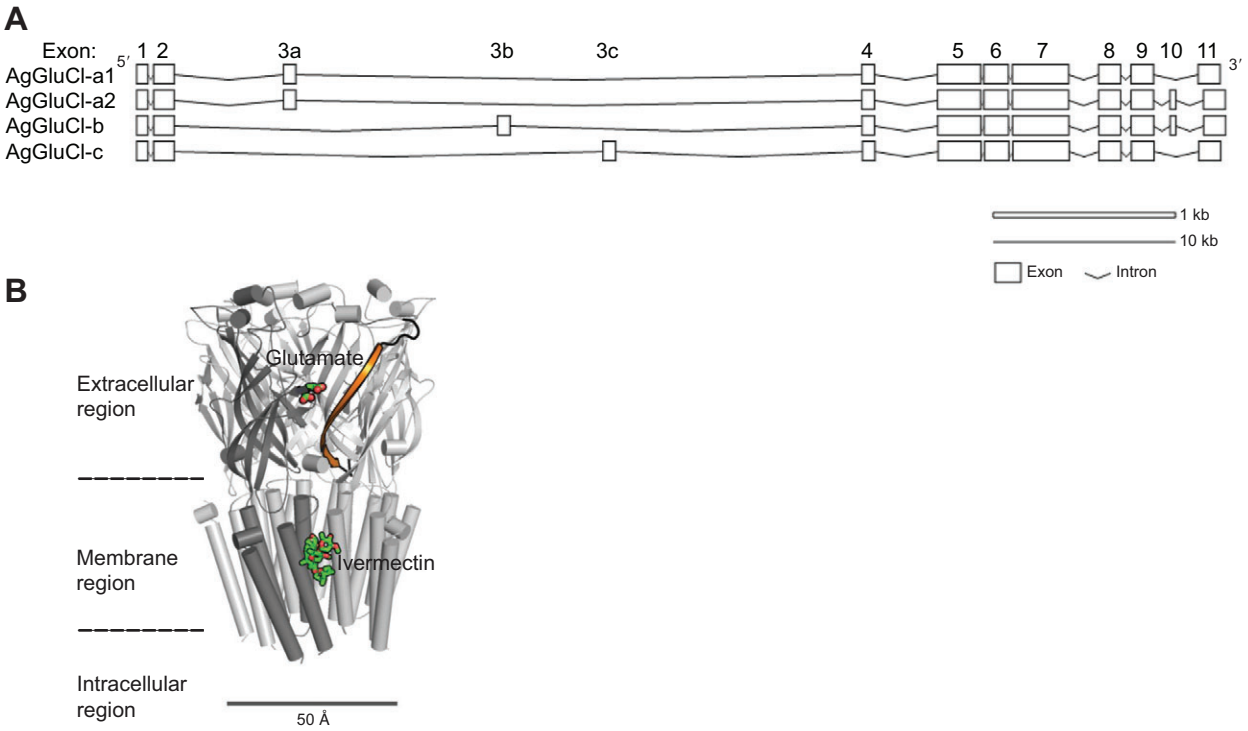

C

```
AgGluCl-a1      MASGHFFWAIFYFACLCSASLANNAKVNFREKEKKILDQILGAGKYDARIRPSGINGTDG 60
AgGluCl-a2      MASGHFFWAIFYFACLCSASLANNAKVNFREKEKKILDQILGAGKYDARIRPSGTNGTDG 60
AgGluCl-b       MASGHFFWAIFYFACLCSASLANNAKVNFREKEKKILDQILGAGKYDARIRPSGINGTDG 60
AgGluCl-c       MASGHFFWAIFYFACLCSASLANNAKVNFREKEKKILDQILGAGKYDARIRPSGINGTDD 60
                ************************************************** ****

AgGluCl-a1      -PAIVRINLFVRSIMTISDIKMEYSVQLTFREQWLDERLKFDDIGGRLKYLTLTEANRVW 119
AgGluCl-a2      -PAIVRINLFVRSIMTISDIKMEYSVQLTFREQWLDERLKFDDIGGRLKYLTLTEANRVW 119
AgGluCl-b       -PAVVRVNIFVRSISKIDDVTMEYSVQLTFREQWLDERLKFDDIGGRLKYLTLTEANRVW 119
AgGluCl-c       KATQVFVNMFLRSISKIDDYKMEYSVQLTFREQWLDERLKFDDIGGRLKYLTLTEANRVW 120
                    *  * * ***  * *  ************************************

AgGluCl-a1      MPDLFFSNEKEGHFHNIIMPNVYIRIFPYGSVLYSIRVSLTLACPMNLKLYPLDRQVCSL 179
AgGluCl-a2      MPDLFFSNEKEGHFHNIIMPNVYIRIFPYGSVLYSIRVSPTLACPTNLKLYPLDRQVCSL 179
AgGluCl-b       MPDLFFSNEKEGHFHNIIMPNVYIRIFPYGSVLYSIRVSLTLACPMNLKLYPLDRQVCSL 179
AgGluCl-c       MPDLFFSNEKEGHFHNIIMPNVYIRIFPYGSVLYSIRVSLTLACPMNLKLYPLDRQVCSL 180
                ************************************ ***** **************

AgGluCl-a1      RMASYGWTTADLVFLWKEGDPVQVVKNLHLPRFTLEKFLTDYCNSKTNTGEYSCLKVDLL 239
AgGluCl-a2      RMASYGWTTADLVFLWKEGDPVQVVKNLHLPRFTLEKFLTDYCNSKTNTGEYSCLKVDLL 239
AgGluCl-b       RMASYGWTTADLVFLWKEGDPVQVVKNLHLPRFTLEKFLTDYCNSKTNTGEYSCLKVDLL 239
AgGluCl-c       RMASYGWTTADLVFLWKEGDPVQVVKNLHLPRFTLEKFLTDYCNSKTNTGEYSCLKVDLL 240
                ************************************************************

                ________________________                ____________________________
AgGluCl-a1      FKREFSYYLIQIYIPCCMLVIVSWVSFWLDQGAVPARVSLGVTTLLTMATQTSGINASLP 299
AgGluCl-a2      FKREFSYYLIQIYIPCCMLVIVSWVSFWLDQGAVPARVSLGVTTLLTMATQTSGINASLP 299
AgGluCl-b       FKREFSYYLIQIYIPCCMLVIVSWVSFWLDQGAVPARVSLGVTTLLTMATQTSGINASLP 299
AgGluCl-c       FKREFSYYLIQIYIPCCMLVIVSWVSFWLDQGAVPARVSLGVTTLLTMATQTSGINASLP 300
                ************************************************************

                ____________________________
AgGluCl-a1      PVSYTKAIDVWTGVCLTFVFGALLEFALVNYASRS-----DMHRENMKKKRREMEQASLD 354
AgGluCl-a2      PVSYTKAIDVWTGVCLTFVFGALLEFALVNYASRS-----DMHRENMKKKRREMEQASLD 354
AgGluCl-b       PVSYTKAIDVWTGVCLTFVFGALLEFALVNYASRSADRAADMHRENMKKKRREMEQASLD 359
AgGluCl-c       PVSYTKAIDVWTGVCLTFVFGALLEFALVNYASRS-----DMHRENMKKKRREMEQASLD 355
                ********************************     ******************

AgGluCl-a1      AASDLLDTDSNATFAMKPLVRHPGDPLALEKLRQCEVHMQAPKRPNCCRSWLSKFPTR-- 412
AgGluCl-a2      AASDLLDTDSNATFAMKPLVRHPGDPLALEKLRQCEVHMQAPKRPNCCRSWLSKFPTSPF 414
AgGluCl-b       AASDLLDTDSNATFAMKPLVRHPGDPLALEKLRQCEVHMQAPKRPNCCRSWLSKFPTSPF 419
AgGluCl-c       AASDLLDTDSNATFAMKPLVRHPGDPLALEKLRQCEVHMQAPKRPNCCRSWLSKFPTR-- 413
                ************************************************************

                                        ____________________
AgGluCl-a1      ---------QCSRSKRIDVISRITFPLVFALFNLVYWSTYLFREEEED 451
AgGluCl-a2      KKVPCLGRGQCSRSKRIDVISRITFPLVFALFNLVYWSTYLFREEEED 462
AgGluCl-b       KKVPCLGRGQCSRSKRIDVISRITFPLVFALFNLVYWSTYLFREEEED 467
AgGluCl-c       ---------QCSRSKRIDVISRITFPLVFALFNLVYWSTYLFREEEED 452
                         ************************************
```

Fig. 1. AgGluCl gene structure, predicted amino acid alignment and homology model. (A) Genetic structure of the *Anopheles gambiae* glutamate-gated chloride channel (AgGluCl) splice isoforms. (B) AgGluCl-a1 homology model with glutamate and ivermectin (IVM) bound. The alternatively spliced portion of the N-terminal extracellular domain (exon 3) is highlighted in orange. (C) ClustalW2 alignment of AgGluCl splice isoform predicted amino acid sequences. Bars denote transmembrane domains; asterisks indicate identical amino acids.

The Journal of Experimental Biology

The Journal of Experimental Biology (2015) 218, 1478-1486 doi:10.1242/jeb.118570

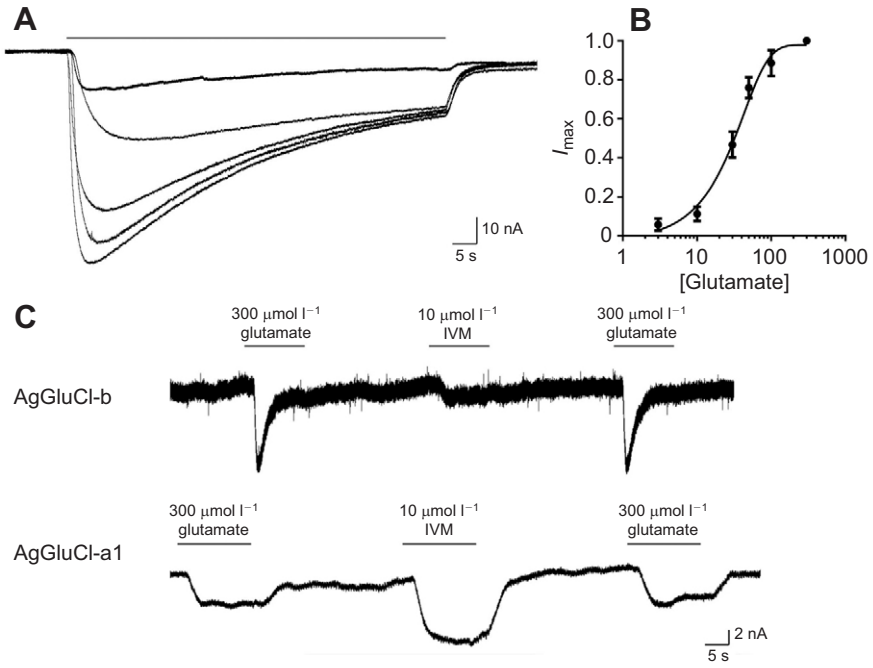

Fig. 2. AgGluCl is activated by glutamate and IVM. (A) Representative currents of AgGluCl-b in response to 10, 30, 50, 100 and 300 μmol l^{-1} glutamate. (B) Glutamate dose–response curve of AgGluCl-b. Data are presented as means and s.d. (C) Representative currents of AgGluCl-a1 and AgGluCl-b in response to glutamate and IVM.

low levels or were completely absent in most tissues until 15 dpe, when AgGluCl-c transcript levels were relatively high (Fig. 3C).

GluCl expression in adult *A. gambiae*

Given that AgGluCl transcripts are abundant in *A. gambiae* head and thorax, we wanted to examine which specific tissues express AgGluCl to begin to understand the physiological role of AgGluCl. We stained sagittal sections of whole adult female (2–4 dpe) mosquitoes for AgGluCl and a neuronal marker (Jan and Jan, 1982) to distinguish neuronal tissue. The anti-AgGluCl IgG was created against the N-terminal extracellular domain of AgGluCl-b and has been shown to bind to multiple AgGluCl isoforms (see the companion paper, Meyers et al., 2015). Immunolabeling showed AgGluCl expression in the antennal segments, Johnston's organ, optic lobe, supraesophageal ganglion and thoracic ganglia (Fig. 4). There were small puncta of AgGluCl staining on antennal segments that could be associated with antennal sensilla (Fig. 4A). The Johnston's organ, a mechanosensory organ in the pedicel associated with audition and flight coordination, has specific AgGluCl staining in the scolopidea (Fig. 4B). AgGluCl is present in the photoreceptors and each layer of the optic lobe, which includes the lamina, medulla and lobula (Fig. 4C). AgGluCl staining was present on neuronal processes as well as cell bodies throughout the supraesophageal ganglion, though it is difficult to distinguish precisely which neuropil contain AgGluCl expression. Lastly, there was AgGluCl staining in all three thoracic ganglia, which contain the motor neurons that control the flight and leg muscles (Fig. 4D).

DISCUSSION

Mass drug administration of IVM is effective at killing *A. gambiae* mosquitoes (Sylla et al., 2010; Alout et al., 2014), inhibiting *P. falciparum* sporogony in *A. gambiae* (Kobylinski et al., 2012) and disrupting malaria parasite transmission in endemic villages (Kobylinski et al., 2011; Alout et al., 2014). Thus, IVM mass drug administration has strong potential to be developed as a novel tool for malaria parasite transmission control. This study is the first to examine the primary target of IVM, GluCl, in any mosquito species.

The cloning of the AgGluCl gene from female *A. gambiae* mRNA revealed four splice isoforms where only three isoforms had previously been predicted (https://www.vectorbase.org) (Megy et al., 2012). These isoforms differ in their splicing of exons 3, 8 and 10. The splicing pattern of exon 3 is similar to GluCl splicing patterns recently discovered in other Dipteran species (Furutani et al., 2014; Kita et al., 2014). This exon encodes the same number of amino acids (22–23 amino acids) and is found in the N-terminal extracellular domain containing loop G of the glutamate binding pocket across *Musca domestica* and *Bombyx mori* (Furutani et al., 2014; Kita et al., 2014). Though this alternatively spliced exon codes for residues involved in glutamate binding, these isoforms have previously been shown to have equal sensitivities to glutamate and IVM in *M. domestica* and *B. mori* (Furutani et al., 2014; Kita et al., 2014). Interestingly, alternative splicing of exon 3 has also been shown to impact heterologous expression of BmGluCl (from *B. mori*) in *X. laevis* oocytes (Furutani et al., 2014). BmGluCl-c had the strongest expression and cell surface density compared with isoforms a and b. Efficient BmGluCl expression required specific amino acid residues at the inter-subunit interface (Thr77, Thr78, Ser80 and Ile82), which are only found on BmGluCl-b and -c but not on isoform a (Furutani et al., 2014). These same residues are conserved in AgGluCl-a1 and -a2, but are not found in AgGluCl-b or -c. This may explain why we had very little success in heterologous expression of AgGluCl-a1 and -b in *X. laevis* oocytes and why the currents were relatively small. We also attempted to express functional AgGluCl isoform in C6/36 cells (derived from *Aedes albopictus*), S2 cells (derived from *D. melanogaster*), Sf9 cells (derived from *Spodoptera frugiperda*) and HEK293 cells (derived from *Homo sapiens*), but only were able to achieve non-functional expression in insect cells (Meyers et al., 2015). This is also highlighted by previous unsuccessful studies attempting to heterologously express functional nicotonic acetylcholine receptors from *A. gambiae* (Jones et al., 2009).

The newly cloned AgGluCl isoforms also contained splicing sites not previously predicted for the gene. These splicing sites occur in the large intracellular loop between transmembrane domains 3 and 4.

The Journal of Experimental Biology (2015) 218, 1478-1486 doi:10.1242/jeb.118570

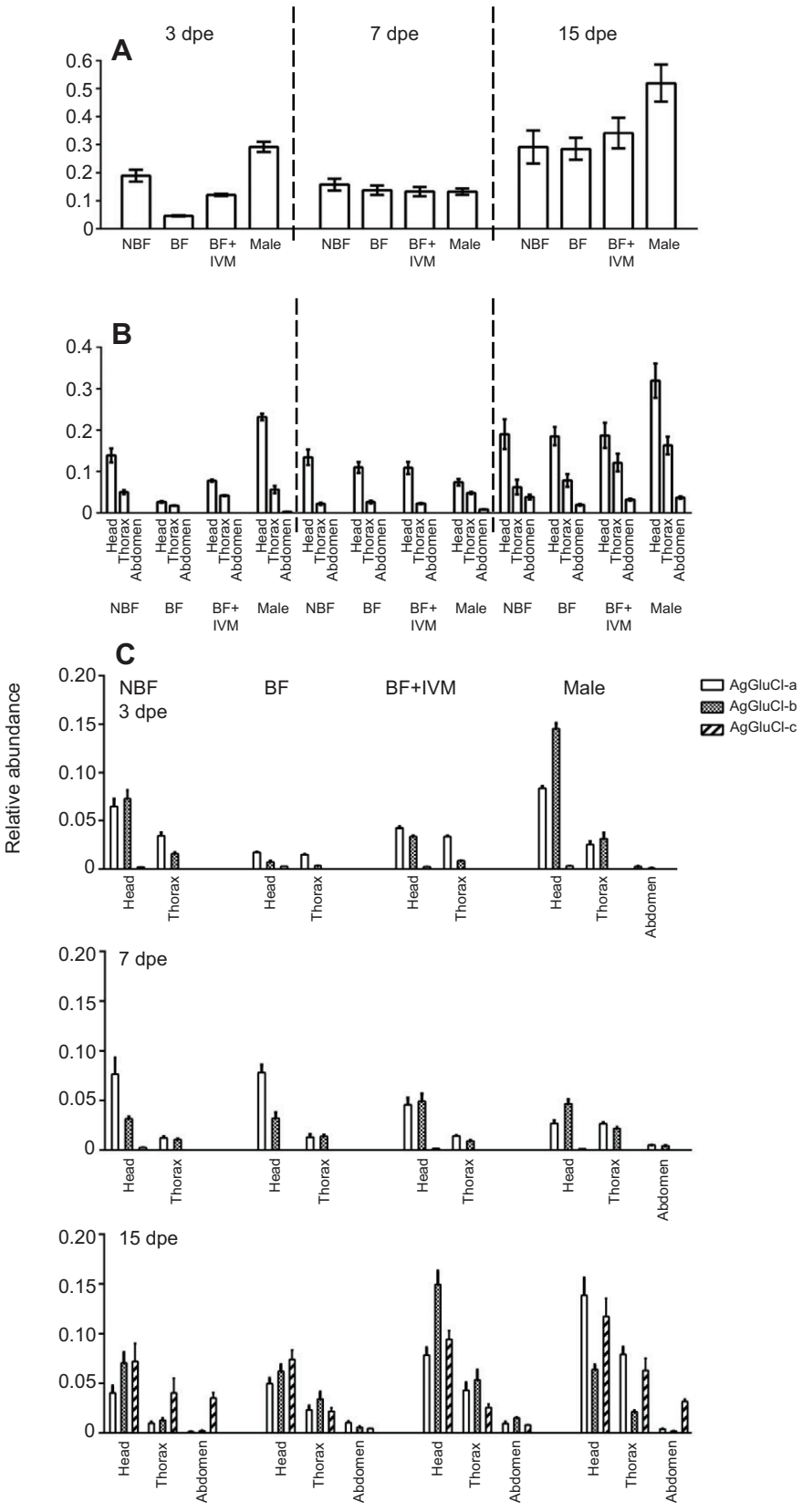

Fig. 3. AgGluCl transcript levels across tissues, age, blood-feeding status and sex. (A,B) *Anopheles gambiae* total AgGluCl transcript levels, relative to ribosomal protein S7 (RPS7), presented by age, blood-feeding status and sex (A) and additionally presented by tissue (B). BF, blood fed; NBF, non-blood fed. (C) AgGluCl splice isoform-specific transcript levels, relative to RPS7, presented by tissue, age, blood-feeding status and sex. Note that the assay could not distinguish between isoforms AgGluCl-a1 and AgGluCl-a2. All data are presented as means and s.d.

The amino acid insertions into the intracellular loop do not affect any potential phosphorylation sites as predicted by NetPhos 2.0 (Blom et al., 1999). The function of this region has been shown to impact channel kinetics and trafficking in other members of the Cys-loop family and provides potential sites for post-translational modifications (Tsetlin et al., 2011; McKinnon et al., 2012). However, it is still unclear how the regions of heterogeneity between isoforms may affect channel activity and expression.

The Journal of Experimental Biology (2015) 218, 1478-1486 doi:10.1242/jeb.118570

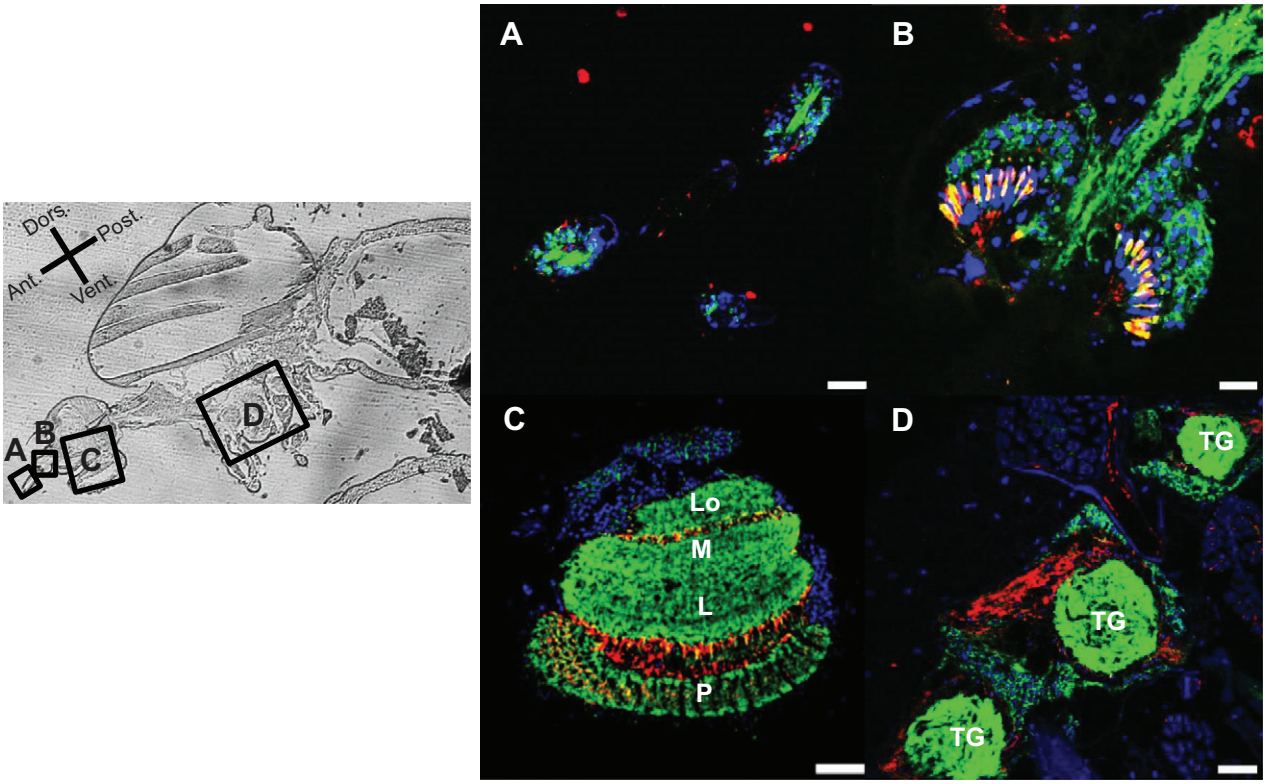

Fig. 4. Representative images of adult, female *A. gambiae* immunoreactive tissues to AgGluCl IgG. Left: differential interference contrast image of a whole, female *A. gambiae* sagittal section outlining the location and orientation of the immunostained images shown on the right. (A) Two antennal segments. Scale bar: 10 µm. (B) Johnston's organ. Scale bar: 10 µm. (C) Head. P, photoreceptors; L, lamina; M, medulla; Lo, lobula. Scale bars: 20 µm. (D) Thoracic ganglia (TG). Scale bar: 50 µm. Red: AgGluCl; green: neuronal marker; blue: DAPI.

AgGluCl-b encodes a rapidly activating glutamate-gated chloride channel sensitive to micromolar concentrations of glutamate and requires cooperative glutamate binding for activity. These characteristics are similar to expressed and native GluCl from *D. melanogaster* and *Locusta migratoria* (Cully et al., 1996; Janssen et al., 2007). Our data show that AgGluCl-b is insensitive to IVM concentrations as high as 10 µmol l^{-1}, which has been shown to activate all IVM-sensitive channels (Lynagh and Lynch, 2012b). However, IVM agonizes AgGluCl-a1 and gates a slowly activating current that exceeds the maximum glutamate response. All AgGluCl isoforms contain the requisite amino acid residues in the IVM binding pocket for IVM-induced activation, including the TM1-Pro and TM3-Gly (supplementary material Fig. S1) (Lynagh and Lynch, 2012a,b). AgGluCl isoforms also contain polar residues hypothesized to coordinate IVM binding on transmembrane domain 2 including Thr-M2-15′ and Arg-M2-19′ (Lynagh and Lynch, 2012b). These two isoforms differ in their splicing of exons 3, 8 and 10, which encode regions in the N-terminal extracellular domain and large intracellular loop between transmembrane domains 3 and 4. It is unclear what residues encoded by these alternatively spliced exons are responsible for IVM sensitivity.

The magnitude of the relative IVM-induced to glutamate-induced peak current for AgGluCl-a1 is similar to *D. melanogaster* and *C. elegans* (Cully et al., 1994, 1996). In our analysis, the IVM response of AgGluCl-a1 was reversible, which has not been observed in GluCls from other organisms. The only other member of the Cys-loop family that is reversibly activated by IVM is the histamine-gated chloride channel from *D. melanogaster* (Zheng et al., 2002). Though IVM does not have persistent activity on AgGluCl-a1 and does not activate AgGluCl-b, it is still highly effective at killing *A. gambiae* (Kobylinski et al., 2010). IVM-induced activity on AgGluCl-a2 and -c splice isoforms is still unknown, as well as potential AgGluCl isoform heteromultimers and AgGluCl-expressing neurons, which may exhibit the more commonly observed persistent IVM-induced activity. Further research comparing AgGluCl isoforms will be necessary to fully understand its physiological role in *A. gambiae* as well as its potential as an insecticide target in regards to insecticide sensitivity and resistance development.

In response to a blood meal, AgGluCl transcript levels decreased modestly at 3 dpe, but were unaffected at 7 dpe and 15 dpe, and we never observed antibody staining intensity differences between non-blood-fed and blood-fed states of 3 dpe mosquitoes (J.I.M. and B.D.F., unpublished results). In this experimental design, the 3 dpe mosquitoes only received one blood meal, whereas 7 and 15 dpe mosquitoes received additional blood meals prior to their final blood meal. This confounding variable could be an alternative explanation for the age-related AgGluCl transcriptional response to a blood meal. Previous microarray data showed that AgGluCl transcripts decrease in response to a blood meal, matching our 3 dpe results, though the researchers do not report the age of the mosquitoes or the number of blood meals received (Marinotti et al., 2006). AgGluCl isoforms are predominately found in the head and thorax. Interestingly, no AgGluCl transcripts were found in the female abdomen until 15 dpe. AgGluCl staining was not observed in the female abdomen, but these experiments were only conducted on 2–4 dpe mosquitoes. It remains unclear what abdominal tissues could be the source of AgGluCl transcripts and what role AgGluCl could play in the mosquito abdomen at this older age.

The Journal of Experimental Biology (2015) 218, 1478-1486 doi:10.1242/jeb.118570

AgGluCl isoform-specific analysis showed predominant expression of AgGluCl-a (isoforms a1 and a2 combined) and AgGluCl-b compared with AgGluCl-c. It is unclear from our analysis what the individual contributions are from AgGluCl-a1 and AgGluCl-a2 transcripts in the overall AgGluCl transcript measurements. We have shown that AgGluCl-b homomers are insensitive to IVM while AgGluCl-a1 homomers are IVM sensitive. Our data suggest that if IVM resistance were to arise in *Anopheles*, it might occur through altered regulation of AgGluCl splicing favoring IVM-insensitive AgGluCl-b transcripts over IVM-sensitive AgGluCl transcripts. When we measured AgGluCl isoform-specific transcription in response to a single IVM-containing blood meal across mosquito tissues and ages, we did not detect a change in the proportion of AgGluCl-b isoforms compared with controls. However, this does not preclude AgGluCl alternative splicing as a potential mechanism for IVM resistance in the field.

To begin to understand what physiological role GluCl has in *A. gambiae*, we stained sagittal slices of whole adult female mosquitoes for AgGluCl and found expression in several vital organs involved in motor and sensory systems. There was significant AgGluCl expression in the thoracic ganglia, which contain the motor neurons that control the flight and leg muscles. GluCl is also expressed in the motor neurons of other invertebrates including *M. domestica* (Kita et al., 2013), *P. americana* (Zhao et al., 2004), *L. migratoria* (Janssen et al., 2007) and *D. melanogaster* larva (Rohrbough and Broadie, 2002). The observed phenotype of mosquitoes that take a blood meal containing IVM is paralysis (Kobylinski et al., 2010). Our data suggest that this paralysis may be due to disruption of GluCl on the motor neurons controlling the leg and flight muscles found in the thoracic ganglia.

We also observed GluCl staining in tissue associated with various sensory systems including the antennal segments, Johnston's organ, optic lobe and supraesophageal ganglion. Chemosensory and thermosensory sensilla are found throughout the antennal segments and play an essential role in host-seeking behavior (Bowen, 1991). GluCl staining was also present in the scolopidia within the Johnston's organ. These hair-like cells are connected to the basal plate of the Johnston's organ, and transduce vibrations in the antenna for audition and flight balance (Gopfert and Robert, 2002; Ignell et al., 2005). Importantly, we have previously reported that sub-lethal doses of IVM impair coordinated flight movement, including increased knockdown and reduced recovery, which could be the result of impairing this sensory organ (Butters et al., 2012). GluCl was present in all three neuropils of the optic lobes, which process visual signals from the compound eye and send projections to the supraesophageal ganglion (Fortini and Rubin, 1991). This is similar to GluCl expression in the optic lobe of *M. domestica* (Kita et al., 2014). Lastly, GluCl expression was present throughout the supraesophageal ganglion. This ganglion is responsible for integrating sensory signals from the antennae and eyes (Ignell et al., 2005; Ignell and Hansson, 2005). GluCl is also expressed in the supraesophageal ganglion of *D. melanogaster* and has been shown to play a key role in circadian rhythms and olfactory processing (McCarthy et al., 2011; Liu and Wilson, 2013). Importantly, hemolymph has been shown to circulate to all of these structures, highlighting the fact that IVM in the hemolymph could affect physiological processes associated with these tissues found relatively far away from the midgut (Boppana and Hillyer, 2014).

As more research is conducted on the potential of IVM mass drug administration for malaria control, it has become essential to understand its target, GluCl, in malaria vectors. This is the first report characterizing GluCl in any mosquito disease vector. We have described the genetic structure, splice isoform-specific transcription, activity and tissue expression of GluCl isoforms in *A. gambiae*. These findings give insight into how IVM affects *Anopheles* physiology and provide a potential mechanism for IVM resistance.

MATERIALS AND METHODS

Mosquitoes

Anopheles gambiae s.s. G3 strain (origin The Gambia) were raised at 28–31°C, 80% relative humidity on a 14 h:10 h light:dark cycle. Larvae were fed ground Tetramin® fish food daily. Adults were provided with water and 10% sucrose solution *ad libitum*. Colony mosquitoes were blood-fed every 3–4 days on defibrinated calf blood. Defibrinated calf blood was prepared by the Colorado Serum Company (Denver, CO, USA) where blood collection protocols are annually reviewed and approved by their IACUC.

AgGluCl cloning

RNA was isolated from 10 female *A. gambiae* mosquitoes using TRIzol® (Invitrogen, Waltham, MA, USA). Contaminating DNA was removed using an RNase-Free DNase Kit (Qiagen, Valencia, CA, USA). A cDNA library was constructed by reverse transcription of isolated RNA with the SuperScript® III Reverse Transcriptase Kit (Invitrogen) using poly-dT and random hexamers. AgGluCl-specific primers were designed for the putative AgGluCl gene from the VectorBase Community Annotation Database (*A. gambiae* PEST strain genomic sequence AGAP001434; Assembly: AgamP4). The following AgGluCl-specific primers were used to probe the cDNA library (5′ to 3′): Fwd1: ATGGCCTCGGGCCATTTCTT; Rev1: TTAGTCCTCCTCCTCTTCGCG; Fwd2: ACGCGTCCCGTTCAGCG-GAT; Rev2: ATCCGCTGAACGGGACGCG. Positive fragments were cloned into pCR4 TOPO TA plasmid (Invitrogen) and sequenced at the Proteomic and Metabolomics Core Facility at Colorado State University.

Gene structure and domain prediction

Signal peptide, transmembrane domains and phosphorylation sites were predicted using SignalP, TMHMM and NetPhos 2.0 on the Center for Biological Sequence Analysis website from the Technical University of Denmark (http://www.cbs.dtu.dk/). The AgGluCl genetic structure was created using Gene Structure Display Server Version 2.0 (http://gsds.cbi.pku.edu.cn/index.php). Amino acid sequence alignments were performed using ClustalW (http://www.ebi.ac.uk/Tools/msa/clustalw2/).

Homology modeling

A homology model for the AgGluCl-a1 isoform was created using MODELLER 9.11 (Eswar et al., 2007). Individual chains of the *C. elegans* crystal structure (3RIF.pdb) were used as comparative models for creating AgGluCl-a1 backbone structures. The AgGluCl-a1 model was truncated to remove disordered termini and loop insertion regions (residues 1–35, 334–415, 448–451). Bound glutamate and ivermectin molecules were added to the homology model through superposition with 3RIF.pdb coordinates. The SHARPEN modeling platform (Loksha et al., 2009) was used to perform combinatorial side chain optimization based on rotamers from the Dunbrack Rotamer Library (Dunbrack and Karplus, 1993).

Quantitative reverse transcription PCR (qRT-PCR) of mosquito tissues

Mosquitoes were aged to 2, 6 and 14 dpe and fed either a normal blood meal or a blood meal containing 11.75 ng ml^{-1} IVM. Mosquitoes at 2 dpe were fed a normal blood meal on day 2, while 7 dpe mosquitoes were fed on days 2 and 6, and 14 dpe mosquitoes were fed on days 2, 6, 10 and 14 to mimic normal blood-feeding patterns. At 24 h after blood feeding, mosquitoes were knocked down at 4°C and sorted into four groups: non-blood-fed females, blood-fed females, IVM blood-fed females and males. Mosquitoes were dissected into head, thorax and abdomen and pooled into three groups of 10 (three biological replicates). RNA was extracted using TRIzol® (Invitrogen), normalized to 25 ng μl^{-1} and stored at −80°C. All blood feeds

and dissections occurred between 14:00 h and 15:00 h to control for circadian rhythms that might affect transcript levels.

qRT-PCR was performed with the SensiMix™ II Probe No-ROX Kit (Bioline, Taunton, MA, USA) to determine AgGluCl isoform-specific transcript levels. AgGluCl primers were designed to pair with sequences on exons 2 and 4 and to amplify the alternatively spliced exons 3a, 3b and 3c (Fwd: GCATCAACGGAACCGACG; Rev: TCGGAACGTAAGCTGT-ACAC; amplicon length: 110 or 113 bp). TaqMan probes were designed against sequences in exons 3a, 3b and 3c to delineate AgGluCl isoforms a1 +a2, b and c (probe A: TCGTTCGAAGCATTATGACCATCAGTGAC; probe B: TGTAAGAAGTATATCTAAAATCGATGACG; probe C: GCC-ACACAAGTGTTCGTCAACATGT). AgGluCl primers and probe specificity and efficiency were validated on serially diluted AgGluCl splice isoforms cloned in the pCR-4 plasmid. All probes utilized FAM fluorophores and TAMRA quenchers. AgGluCl transcript levels were measured relative to ribosomal protein S7 (RPS7 Fwd: AGCAGCTACAGCACTTGATTATTGG; Rev: AGCAGCTACAGCACTTGATTATTGG; Probe: CCCGATTTCTCC-GATCTTTCACATTCCA) (Blandin et al., 2004). All reactions were performed in technical duplicate with each well containing 25 ng of RNA. All plates contained a no-template control and positive controls of each AgGluCl splice isoform. AgGluCl splice isoform transcript levels were compared using 2-way ANOVA with Tukey's *post hoc* analysis.

In vitro transcription and oocyte expression

AgGluCl cDNA was cloned into the pGEM-HE plasmid. The plasmid was linearized using the BspQ1 restriction enzyme. Capped mRNA was synthesized using the mMessage mMachine® T7 Ultra Kit (Ambion, Grand Island, NY, USA). Stage 4–5 *Xenopus laevis* oocytes (EcoCyte Bioscience, Austin, TX, USA) were maintained at 18°C in Barth's solution [87.6 mmol l^{-1} NaCl, 2.4 mmol l^{-1} $NaHCO_3$, 1.1 mmol l^{-1} KCl, 0.32 mmol l^{-1} $Ba(NO_3)_2$, 0.4 mmol l^{-1} $BaCl_2$, 0.8 mmol l^{-1} $MgCl_2$, 15 mmol l^{-1} Hepes, pH 7.6]. Oocytes were injected with 46 nl of mRNA (500 ng μl^{-1}) using a Drummond Nanoject (Drummond Scientific, Broomall, PA, USA) and micropipettes with a tip <10 µm in diameter. Oocytes were incubated in Barth's solution for 72–120 h at 18°C before recording.

Oocyte electrophysiology

Oocytes were recorded using two-electrode voltage clamp (GeneClamp 500B) held at −80 mV. Oocytes were continuously perfused at a rate of 4 ml min^{-1} via a peristaltic pump. The extracellular solution contained Barth's solution plus glutamate or IVM (Sigma-Aldrich, St Louis, MO, USA; a mixture of two submoieties B1a and B1b, primarily containing B1a) as specified. IVM solutions were made from a 10 mg ml^{-1} IVM stock dissolved in DMSO. Control solutions contained equal volumes of DMSO, which never exceeded 1% and had no effect on the oocytes. Solution exchange was controlled via the BPS-8 Valve Control System (ALA Scientific, Farmingdale, NY, USA) and electronic valves. Electrodes of 1–5 MΩ were filled with 1 mol l^{-1} $CsCl_2$ and 5 mmol l^{-1} EGTA pH 7.5 to prevent activation of endogenous calcium-activated chloride channels. As a negative control, we performed two-electrode patch clamp on non-injected and water-injected oocytes, which never resulted in glutamate- or IVM-induced currents. As a positive control, we injected oocytes with a mammalian glutamate-gated cation channel (GluA1) (Partin, 2001) and successfully measured glutamate-induced currents. Current responses were acquired using an HP ProBook 6460b with an Instrutech ITC-16 interface under the control of AxoGraph X acquisition software. A dose–response curve was fitted to the data using the Hill equation:

$$I_{\max} = \frac{1}{1 + \left(\frac{EC_{50}}{[L]}\right)^{H}}, \quad (1)$$

where I_{max} is the maximal response, $[L]$ is the ligand concentration, EC_{50} is the ligand concentration for the half maximal response and H is the Hill coefficient. The Hill coefficient is the number of ligands required to activate the channel. Five biological replicates were tested for each measurement.

Immunohistochemistry

Samples were prepared from female blood-fed *A. gambiae* aged 2–4 dpe. Twenty-four hours after blood feeding, 24 engorged females were knocked down at 4°C and injected intrathoracically with 46 nl of 4% paraformaldehyde (Drummond Nanoject). Specimens were briefly washed in 70% ethanol before overnight fixation in 4% paraformaldehyde at 4°C. After fixation, specimens were paraffin embedded, cut into 5 µm thick slices and mounted onto slides (Colorado HistoPrep, Fort Collins, CO, USA). Slides were heated at 65°C for 10 min and treated with xylene to remove the paraffin layer, then re-hydrated with graded washes in ethanol and PBS. Specimens were treated with graded washes of methanol and PBS to reduce autofluorescence. Slides were blocked for 2 h with 10% non-fat dry milk and 0.1% Triton-X in PBS. Primary antibody staining consisted of 1:500 rabbit anti-AgGluCl IgG (prepared by GenScript, Piscataway, NJ, USA) and 1:500 goat anti-HRP antibodies to stain neuronal tissue (Jan and Jan, 1982) (Jackson ImmunoResearch Laboratories, West Grove, PA, USA) and incubated overnight at 4°C. Rabbit-derived polyclonal anti-AgGluCl IgG was created against the N-terminal extracellular domain of AgGluCl-b by GenScript. Antibody specificity was verified through ELISA, western blot and immunostaining of C6/36 cells transfected with AgGluCl-a1 and AgGluCl-b (Meyers et al., 2015). Specimens were washed with 0.05% Tween-20 Tris-based buffer solution (TTBS) and then incubated with 1:1000 donkey anti-rabbit Alexa 555 (Invitrogen) and 1:1000 donkey anti-goat Alexa 488 (Invitrogen) for 3 h at room temperature. Slides were mounted with VectaShield® containing DAPI (Vector Laboratories, Burlingame, CA, USA). Negative controls underwent the same procedure, but substituted histidine affinity-purified polyclonal rabbit IgG from non-immunized rabbits as the primary antibody.

Acknowledgements

This work is dedicated to the late Ines Marques da Silva for her assistance with this project. We thank T. Burton and J. Seaman for their laboratory assistance.

Competing interests

The authors declare no competing or financial interests.

Author contributions

J.I.M. and B.D.F. conceived the study. J.I.M., B.D.F., K.M.P. and C.D.S. designed the experiments. J.I.M., M.G., W.K. and L.B.J. performed the experiments. J.I.M., B.D.F., W.C.B. IV and K.M.P. analyzed the data. J.I.M. and B.D.F. wrote the manuscript.

Funding

These studies were supported by the National Institutes of Health [R01AI94349-01A1 to B.D.F.] and the Colorado State University Infectious Disease Supercluster [1-32613 to B.D.F. and K.M.P.]. Deposited in PMC for release after 12 months.

Supplementary material

Supplementary material available online at
http://jeb.biologists.org/lookup/suppl/doi:10.1242/jeb.118570/-/DC1

References

Alout, H., Krajacich, B. J., Meyers, J. I., Grubaugh, N. D., Brackney, D. E., Kobylinski, K. C., Diclaro, J. W., II, Bolay, F. K., Fakoli, L. S., Diabaté, A. et al. (2014). Evaluation of ivermectin mass drug administration for malaria transmission control across different West African environments. *Malar. J.* **13**, 417.

Blandin, S., Shiao, S.-H., Moita, L. F., Janse, C. J., Waters, A. P., Kafatos, F. C. and Levashina, E. A. (2004). Complement-like protein TEP1 is a determinant of vectorial capacity in the malaria vector *Anopheles gambiae*. *Cell* **116**, 661-670.

Blom, N., Gammeltoft, S. and Brunak, S. (1999). Sequence and structure-based prediction of eukaryotic protein phosphorylation sites. *J. Mol. Biol.* **294**, 1351-1362.

Boppana, S. and Hillyer, J. F. (2014). Hemolymph circulation in insect sensory appendages: functional mechanics of antennal accessory pulsatile organs (auxiliary hearts) in the mosquito *Anopheles gambiae*. *J. Exp. Biol.* **217**, 3006-3014.

Bowen, M. F. (1991). The sensory physiology of host-seeking behavior in mosquitoes. *Annu. Rev. Entomol.* **36**, 139-158.

Brown, D. D. R., Siddiqui, S. Z., Kaji, M. D. and Forrester, S. G. (2012). Pharmacological characterization of the *Haemonchus contortus* GABA-gated chloride channel, Hco-UNC-49: modulation by macrocyclic lactone anthelmintics and a receptor for piperazine. *Vet. Parasitol.* **185**, 201-209.

Butters, M. P., Kobylinski, K. C., Deus, K. M., da Silva, I. M., Gray, M., Sylla, M. and Foy, B. D. (2012). Comparative evaluation of systemic drugs for their effects against *Anopheles gambiae*. *Acta Trop.* **121**, 34-43.

Cully, D. F., Vassilatis, D. K., Liu, K. K., Paress, P. S., Van der Ploeg, L. H. T., Schaeffer, J. M. and Arena, J. P. (1994). Cloning of an avermectin-sensitive glutamate-gated chloride channel from *Caenorhabditis elegans*. *Nature* **371**, 707-711.

Cully, D. F., Paress, P. S., Liu, K. K., Schaeffer, J. M. and Arena, J. P. (1996). Identification of a *Drosophila melanogaster* glutamate-gated chloride channel sensitive to the antiparasitic agent avermectin. *J. Biol. Chem.* **271**, 20187-20191.

Dunbrack, R. L., Jr and Karplus, M. (1993). Backbone-dependent rotamer library for proteins Application to side-chain prediction. *J. Mol. Biol.* **230**, 543-574.

Eswar, N., Webb, B., Marti-Renom, M. A., Madhusudhan, M. S., Eramian, D., Shen, M.-Y., Pieper, U. and Sali, A. (2007). Comparative protein structure modeling using MODELLER. *Curr. Protoc. Protein Sci.* Chapter 2, Unit 2 9.

Fortini, M. E. and Rubin, G. M. (1991). The optic lobe projection pattern of polarization-sensitive photoreceptor cells in *Drosophila melanogaster*. *Cell Tissue Res.* **265**, 185-191.

Furutani, S., Ihara, M., Nishino, Y., Akamatsu, M., Jones, A. K., Sattelle, D. B. and Matsuda, K. (2014). Exon 3 splicing and mutagenesis identify residues influencing cell surface density of heterologously expressed silkworm (*Bombyx mori*) glutamate-gated chloride channels. *Mol. Pharmacol.* **86**, 686-695.

Gopfert, M. C. and Robert, D. (2002). The mechanical basis of *Drosophila* audition. *J. Exp. Biol.* **205**, 1199-1208.

Hibbs, R. E. and Gouaux, E. (2011). Principles of activation and permeation in an anion-selective Cys-loop receptor. *Nature* **474**, 54-60.

Ignell, R. and Hansson, B. S. (2005). Projection patterns of gustatory neurons in the suboesophageal ganglion and tritocerebrum of mosquitoes. *J. Comp. Neurol.* **492**, 214-233.

Ignell, R., Dekker, T., Ghaninia, M. and Hansson, B. S. (2005). Neuronal architecture of the mosquito deutocerebrum. *J. Comp. Neurol.* **493**, 207-240.

Jan, L. Y. and Jan, Y. N. (1982). Antibodies to horseradish peroxidase as specific neuronal markers in *Drosophila* and in grasshopper embryos. *Proc. Natl. Acad. Sci. USA* **79**, 2700-2704.

Janssen, D., Derst, C., Buckinx, R., Van den Eynden, J., Rigo, J.-M. and Van Kerkhove, E. (2007). Dorsal unpaired median neurons of *Locusta migratoria* express ivermectin- and fipronil-sensitive glutamate-gated chloride channels. *J. Neurophysiol.* **97**, 2642-2650.

Janssen, D., Derst, C., Rigo, J. M. and Van Kerkhove, E. (2010). Cys-loop ligand-gated chloride channels in dorsal unpaired median neurons of *Locusta migratoria*. *J. Neurophysiol.* **103**, 2587-2598.

Jones, A. K., Buckingham, S. D., Brown, L. A. and Sattelle, D. B. (2009). Alternative splicing of the *Anopheles gambiae* nicotinic acetylcholine receptor, Agamalphabeta9, generates both alpha and beta subunits. *Invert. Neurosci.* **9**, 77-84.

Kita, T., Ozoe, F., Azuma, M. and Ozoe, Y. (2013). Differential distribution of glutamate- and GABA-gated chloride channels in the housefly *Musca domestica*. *J. Insect Physiol.* **59**, 887-893.

Kita, T., Ozoe, F. and Ozoe, Y. (2014). Expression pattern and function of alternative splice variants of glutamate-gated chloride channel in the housefly *Musca domestica*. *Insect Biochem. Mol. Biol.* **45**, 1-10.

Kobylinski, K. C., Deus, K. M., Butters, M. P., Hongyu, T., Gray, M., da Silva, I. M., Sylla, M. and Foy, B. D. (2010). The effect of oral anthelmintics on the survivorship and re-feeding frequency of anthropophilic mosquito disease vectors. *Acta Trop.* **116**, 119-126.

Kobylinski, K. C., Sylla, M., Chapman, P. L., Sarr, M. D. and Foy, B. D. (2011). Ivermectin mass drug administration to humans disrupts malaria parasite transmission in Senegalese villages. *Am. J. Trop. Med. Hyg.* **85**, 3-5.

Kobylinski, K. C., Foy, B. D. and Richardson, J. H. (2012). Ivermectin inhibits the sporogony of *Plasmodium falciparum* in *Anopheles gambiae*. *Malar. J.* **11**, 381.

Liu, W. W. and Wilson, R. I. (2013). Glutamate is an inhibitory neurotransmitter in the *Drosophila* olfactory system. *Proc. Natl. Acad. Sci. USA* **110**, 10294-10299.

Loksha, I. V., Maiolo, J. R., III, Hong, C. W., Ng, A. and Snow, C. D. (2009). SHARPEN-systematic hierarchical algorithms for rotamers and proteins on an extended network. *J. Comput. Chem.* **30**, 999-1005.

Lynagh, T. and Lynch, J. W. (2012a). Molecular mechanisms of Cys-loop ion channel receptor modulation by ivermectin. *Front. Mol. Neurosci.* **5**, 60.

Lynagh, T. and Lynch, J. W. (2012b). Ivermectin binding sites in human and invertebrate Cys-loop receptors. *Trends Pharmacol. Sci.* **33**, 432-441.

Marinotti, O., Calvo, E., Nguyen, Q. K., Dissanayake, S., Ribeiro, J. M. C. and James, A. A. (2006). Genome-wide analysis of gene expression in adult Anopheles gambiae. *Insect Mol. Biol.* **15**, 1-12.

McCarthy, E. V., Wu, Y., deCarvalho, T., Brandt, C., Cao, G. and Nitabach, M. N. (2011). Synchronized bilateral synaptic inputs to *Drosophila melanogaster* neuropeptidergic rest/arousal neurons. *J. Neurosci.* **31**, 8181-8193.

McCavera, S., Rogers, A. T., Yates, D. M., Woods, D. J. and Wolstenholme, A. J. (2009). An ivermectin-sensitive glutamate-gated chloride channel from the parasitic nematode *Haemonchus contortus*. *Mol. Pharmacol.* **75**, 1347-1355.

McKinnon, N. K., Bali, M. and Akabas, M. H. (2012). Length and amino acid sequence of peptides substituted for the 5-HT3A receptor M3M4 loop may affect channel expression and desensitization. *PLoS ONE* **7**, e35563.

Megy, K., Emrich, S. J., Lawson, D., Campbell, D., Dialynas, E., Hughes, D. S. T., Koscielny, G., Louis, C., MacCallum, R. M., Redmond, S. N. et al. (2012). VectorBase: improvements to a bioinformatics resource for invertebrate vector genomics. *Nucleic Acids Res.* **40**, D729-D734.

Meyers, J. I., Gray, M. and Foy, B. D. (2015). Mosquitocidal properties of IgG targeting the glutamate-gated chloride channel in three mosquito disease vectors (Diptera: Culicidae). *J. Exp. Biol.* **218**, 1487-1495.

Moreno, Y., Nabhan, J. F., Solomon, J., Mackenzie, C. D. and Geary, T. G. (2010). Ivermectin disrupts the function of the excretory-secretory apparatus in microfilariae of *Brugia malayi*. *Proc. Natl. Acad. Sci. USA* **107**, 20120-20125.

Õmura, S. (2008). Ivermectin: 25 years and still going strong. *Int. J. Antimicrob. Agents* **31**, 91-98.

Ouedraogo, A. L., Bastiaens, G. J. H., Tiono, A. B., Guelbeogo, W. M., Kobylinski, K. C., Ouedraogo, A., Barry, A., Bougouma, E. C., Nebie, I., Ouattara, M. S. et al. (2014). Efficacy and safety of the mosquitocidal drug ivermectin to prevent malaria transmission after treatment: a double-blind, randomized, clinical trial. *Clin. Infect. Dis.* **60**, 357-365.

Partin, K. M. (2001). Domain interactions regulating AMPA receptor desensitization. *J. Neurosci.* **21**, 1939-1948.

Ranson, H., N'Guessan, R., Lines, J., Moiroux, N., Nkuni, Z. and Corbel, V. (2011). Pyrethroid resistance in African Anopheline mosquitoes: what are the implications for malaria control? *Trends Parasitol.* **27**, 91-98.

Rohrbough, J. and Broadie, K. (2002). Electrophysiological analysis of synaptic transmission in central neurons of *Drosophila* larvae. *J. Neurophysiol.* **88**, 847-860.

Schnizler, K., Saeger, B., Pfeffer, C., Gerbaulet, A., Ebbinghaus-Kintscher, U., Methfessel, C., Franken, E.-M., Raming, K., Wetzel, C. H., Saras, A. et al. (2005). A novel chloride channel in *Drosophila* melanogaster is inhibited by protons. *J. Biol. Chem.* **280**, 16254-16262.

Sylla, M., Kobylinski, K. C., Gray, M., Chapman, P. L., Sarr, M. D., Rasgon, J. L. and Foy, B. D. (2010). Mass drug administration of ivermectin in south-eastern Senegal reduces the survivorship of wild-caught, blood fed malaria vectors. *Malar. J.* **9**, 365.

Trape, J.-F., Tall, A., Diagne, N., Ndiath, O., Ly, A. B., Faye, J., Dieye-Ba, F., Roucher, C., Bouganali, C., Badiane, A. et al. (2011). Malaria morbidity and pyrethroid resistance after the introduction of insecticide-treated bednets and artemisinin-based combination therapies: a longitudinal study. *Lancet Infect. Dis.* **11**, 925-932.

Tsetlin, V., Kuzmin, D. and Kasheverov, I. (2011). Assembly of nicotinic and other Cys-loop receptors. *J. Neurochem.* **116**, 734-741.

Zhao, X., Salgado, V. L., Yeh, J. Z. and Narahashi, T. (2004). Kinetic and pharmacological characterization of desensitizing and non-desensitizing glutamate-gated chloride channels in cockroach neurons. *Neurotoxicology* **25**, 967-980.

Zheng, Y., Hirschberg, B., Yuan, J., Wang, A. P., Hunt, D. C., Ludmerer, S. W., Schmatz, D. M. and Cully, D. F. (2002). Identification of two novel *Drosophila melanogaster* histamine-gated chloride channel subunits expressed in the eye. *J. Biol. Chem.* **277**, 2000-2005.

Fig. S1. ClustalW alignment of AgGluCl amino acid sequences with *D. melanogaster* GluCl (DmGluCl) and *C. elegans* GluCl (CeGluCl). Black bar denotes transmembrane domains. (*) glutamate binding residues; (#) critical residues for ivermectin binding.